

NACA RM L62H12

7360



TECH LIBRARY KAFB, NM

014443

RESEARCH MEMORANDUM

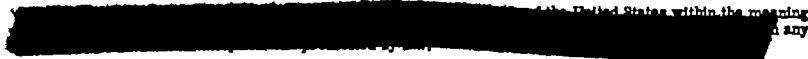
LOW-LIFT BUFFET CHARACTERISTICS OBTAINED FROM FLIGHT
 TESTS OF UNSWEPT THIN INTERSECTING SURFACES AND
 OF THICK 35° SWEPTBACK SURFACES

By Homer P. Mason

Langley Aeronautical Laboratory
 Langley Field, Va.

**RECEIPT SIGNATURE
 REQUIRED**

CLASSIFIED DOCUMENT



**NATIONAL ADVISORY COMMITTEE
 FOR AERONAUTICS**

WASHINGTON

January 16, 1953

CONFIDENTIAL

Classification changed to: Unclassified
By Authority: NASA Tech Rep Announcement
89 8 SEP 55

By.....

GRADE OF OFFICER (OR RANK CHANGE)

NK

16 Apr 61
DATE

CONFIDENTIAL

TECH LIBRARY KAFB, NM



0144443

NATIONAL ADVISORY COMMITTEE FOR AERONAUTICS

RESEARCH MEMORANDUM

LOW-LIFT BUFFET CHARACTERISTICS OBTAINED FROM FLIGHT
TESTS OF UNSWEPT THIN INTERSECTING SURFACES AND
OF THICK 35° SWEEPBACK SURFACES

By Homer P. Mason

SUMMARY

Two rocket-propelled research models have been flight-tested to determine the effect of the intersection of thin aerodynamic surfaces and the effect of moderate sweepback of thick aerodynamic surfaces on low-lift buffeting. Data from the test of a configuration having 6-percent-thick unswept surfaces mounted in a conventional intersecting-tail arrangement on a clean body show that low-lift buffeting and a change in trim normal-force coefficient were encountered simultaneously at transonic speeds. Low-lift buffeting may be induced by the interference effects of thin intersecting surfaces and local interference effects on an intersecting-tail arrangement may be partially responsible for persistent transonic trim changes. Data from this test indicate an increase in drag coefficient over that of a comparable symmetrical configuration. Data from the test of a configuration having 12-percent-thick surfaces swept back 35° also show that low-lift buffeting and a change in trim normal-force coefficient occurred simultaneously at transonic speeds. Sweeping back a thick surface reduces the buffet intensity, normal-force trim change, and total drag coefficient. Buffet intensity data from the two tests are presented.

INTRODUCTION

Buffet boundaries obtained from tests of various aircraft (refs. 1 to 5) indicate the importance in the buffet phenomenon of such parameters as Mach number, lift coefficient, and airfoil thickness ratio. Little information is available, however, concerning the effects of features such as the intersection of aerodynamic surfaces or the variation of airfoil plan form. As an extension of the investigation of reference 1, flight tests have been conducted at the Langley Pilotless

CONFIDENTIAL

HMDC 146

Aircraft Research Station at Wallops Island, Va., by the rocket-propelled-model technique to determine whether the intersection of thin wings could cause low-lift buffeting and whether moderate sweepback of a thick wing would eliminate low-lift buffeting. The purpose of this paper is to present and to discuss the data obtained from these tests.

SYMBOLS

c	wing chord, ft
t/c	thickness ratio, percent chord
c_r	chord of intersection of vertical and horizontal surfaces, ft
R	Reynolds number, based on the mean aerodynamic chord of vertical surfaces
M	Mach number
p	rolling velocity, radians/sec
V	free-stream velocity, feet/sec
b	wing span, ft
$pb/2V$	wing-tip helix angle, radians
q	free-stream dynamic pressure, lb/sq ft
S_h	total area of horizontal surface, sq ft
S_v	total area of vertical surface, sq ft
S_t	total exposed area, sq ft
N	trim normal force, lb
$C_{N_{trim}}$	trim normal-force coefficient, N/qS_h
Y	trim side force, lb
$C_{Y_{trim}}$	trim side-force coefficient, Y/qS_v
D	drag, lb

C_D	total drag coefficient, D/qS_t
P_s	local static pressure, lb/sq ft
P_o	free-stream static pressure, lb/sq ft
$(P_s - P_o)/q$	pressure coefficient

MODELS AND TESTS

Surfaces of aspect ratio 4.0 and taper ratio 0.5 were mounted as tails on the basic test vehicle of reference 1 to obtain the desired configurations. (See figs. 1 to 3.) The vertical surfaces of both models had NACA 65A006 airfoil sections, zero sweep of the 0.6-chord line, and were built to the same dimensions. Because the vertical surfaces had the same dimensions, Reynolds numbers (fig. 4) are based on the mean aerodynamic chord of these surfaces (0.619 foot based on total area).

Models

Intersecting-surface configuration.- Horizontal surfaces having NACA 65A006 airfoil sections and zero sweep of the 0.6-chord line were mounted on the upper vertical surface of this model with the root chord coincident with the chord of intersection and $0.25c_r$ above the fuselage at the leading edge (fig. 1). All surfaces were of wood-core construction with cycle-welded skin and trailing-edge inserts of aluminum alloy. The intersection was braced with four cross-shaped aluminum alloy stiffeners, one arm of which extended between the surface inlays of each wing. The first-bending natural frequencies of these surfaces were measured and were found to be 120 cycles per second for the horizontal surface, 135 cycles per second for the upper (intersecting) vertical surface, and 115 cycles per second for the lower vertical surface. Second-bending natural frequencies of all surfaces were of the order of 350 cycles per second. The rigidity of this type construction, coupled with previous experience, made the occurrence of flutter extremely unlikely in the present test.

Swept-surface configuration.- Horizontal surfaces having NACA 651A012 airfoil sections normal to the 0.6-chord line and 35° sweepback of the 0.25-chord line were mounted in the plane of the model center line (fig. 2.) These surfaces were obtained by rotating the 12-percent-thick surfaces of reference 1 backward 28° about the root-quarter-chord point and extending the span to maintain the aspect ratio of the unswept

surfaces. The resulting streamwise thickness was approximately 10.4 percent. These surfaces were of wood-core construction with cycle-welded skin and trailing-edge inserts of aluminum alloy. First-bending natural frequencies were approximately 120 cycles per second for the swept horizontal surfaces and 115 cycles per second for the unswept vertical surfaces. The estimated flutter speed was well above the maximum velocity reached in the test of this model.

Instrumentation

Both models were instrumented to measure normal and longitudinal accelerations as in reference 1. Normal accelerometers were located in each model at the 44-percent body station and in the body under the 25-percent chord of the test surfaces. In addition, a transverse accelerometer was located in the body at the 25-percent chord of the vertical surfaces to measure buffet frequencies and amplitude in the transverse plane. A static-pressure orifice was located midway between the fuselage and the horizontal surface, at the 63-percent chord of the vertical surface, of the model having intersecting surfaces (fig. 1(b)) and on the body, at approximately the maximum diameter, of the swept-surface configuration.

Tests

Both models were accelerated to a Mach number of approximately 0.8 by a high-performance booster-rocket motor and accelerated slowly after booster separation to a peak Mach number of approximately 1.4 by a built-in sustainer rocket motor. Accelerometer and pressure data were measured continuously during the entire flight, and transmitted to the ground station by means of the NACA telemetering system. The accelerometer records during the power-on part of the flight test contain random vibrations which cannot be definitely identified and were not considered in this analysis. Velocity and flight-path data were obtained from CW Doppler and tracking radar, roll data from spinsonde recorders, and atmospheric data from radiosondes released after each flight.

RESULTS AND DISCUSSION

Reproductions of portions of the telemeter records of normal and transverse accelerations at the tail of each model are shown in figures 5 and 6. The irregular nature of the buffet oscillations and the change in level of normal and transverse accelerations are indicated on these figures. The Mach number boundaries, indicated on figures 5 and 6 and used elsewhere in this paper, represent the points at which a definite

increase in the intensity of the oscillating accelerometer trace can be detected and may or may not define the actual boundary for initial buffeting. It is estimated, however, that changes in normal-force coefficient of the order of 0.01 are detectable on the accelerometer records. Average amplitude-response factors for the accelerometer-recorder system were estimated to be approximately 0.36 for the intersecting-surface configuration and approximately 0.5 for the swept-surface configuration at the frequencies encountered in these tests.

Buffeting

Intersecting-surface configuration.- Low-lift buffeting occurred between Mach numbers of 0.87 and 0.99 in both planes of the 6-percent-thick intersecting surfaces (fig. 5). The maximum buffet amplitude was approximately $\pm 1.5g$, $\Delta C_N = \pm 0.09$. Buffet frequencies varied irregularly between 100 and 150 cycles per second. It is considered probable that these frequencies are the resultants of the first-bending natural frequencies of the horizontal and vertical surfaces.

References 1 and 3 show that 6-percent-thick unswept surfaces should not encounter transonic low-lift buffeting when symmetrically mounted on a clean body. Comparison of the trim-lift coefficients of the model having 7-percent-thick surfaces (ref. 1) and the model of the present test indicates that the effect of lift coefficient on the occurrence of buffeting in the present test may be neglected. It may be concluded, therefore, that the low-lift buffeting encountered in the present test was induced by the interference due to the intersection of relatively thin aerodynamic surfaces. The possibility, however, that the low-lift buffeting encountered may have been due to interference between the horizontal surface and the body should not be completely overlooked.

Swept-surface configuration.- Low-lift buffeting occurred between Mach numbers of 0.91 and 1.00 on the 12-percent-thick surfaces swept back 35° , (fig. 6). The maximum buffet amplitude was approximately $\pm 1.0g$, $\Delta C_N = \pm 0.05$. Buffet frequencies correspond to the natural frequency of the sweptback surfaces in first bending - approximately 120 cycles per second.

Although no definite buffet boundaries are available for comparable swept surfaces, data from this test agree well with the few test points of reference 5. The surfaces used in the present test were similar to the 12-percent-thick surfaces of reference 1 except for the angle of sweep and the streamwise thickness. Since the model having 12-percent-thick unswept surfaces (ref. 1) and the model used in the present test were both at zero-lift conditions at the onset of buffeting, it may be concluded that 35° of sweep and a reduction of thickness from 12.0- to 10.4-percent chord reduced the maximum buffet amplitude approximately 50 percent and delayed the onset of buffeting from approximately 0.88 to 0.91 Mach number.

Trim Changes

Intersecting surface configuration.- Trim normal-force coefficients calculated from normal accelerometers in the nose and tail, trim side-force coefficients estimated from the transverse accelerometer in the tail, and trim wing-helix angles are shown as a function of Mach number on figures 7 and 8 for both models. The model having intersecting surfaces experienced an abrupt change of trim normal-force coefficient simultaneously with the occurrence of buffeting (fig. 7) and a change in level of the trim normal-force coefficient from approximately 0.03 at subsonic speeds to 0.08 at supersonic speeds. No wing dropping was evident (fig. 7) and only a mild change in trim side-force coefficient was experienced (fig. 8).

Static-pressure coefficients measured on the vertical surface between the horizontal surface and the body of this model, and static-pressure coefficients measured at the maximum diameter of a similar body (model having 12-percent-thick sweptback wings) are shown in figure 9. The pressure at the maximum diameter has been measured on another model having the same body shape (ref. 1) and shows excellent agreement with the curve shown in the present tests. Thus, it is believed that the large pressure change occurring between the horizontal surfaces and the body in the present test was a local phenomenon and not an effect of an upstream disturbance and that this local disturbance was partially responsible for the change of trim normal-force coefficient encountered in the present test. It is evident that this pressure change was nearly symmetrical about the vertical plane since only a mild change in side force and no wing dropping were encountered.

Swept-surface configuration.- The trim normal-force coefficients (fig. 7) and the trim side-force coefficients (fig. 8) show only mild trim changes for the model having 12-percent-thick surfaces swept back 35°. It is of interest to note that the change of trim normal-force coefficient due largely to the 12-percent-thick sweptback surfaces was of the same order as the change of side-force coefficient due largely to the 6-percent-thick unswept vertical surfaces and was less severe than that due to the 12-percent-thick unswept surfaces of reference 1. Changes of trim normal-force coefficient occurred simultaneously with the occurrence of buffeting as reported in reference 1 for the unswept 12-percent-thick surface. No wing dropping data were obtained in this test due to failure of the equipment for measuring rate of roll.

Buffet Intensity

There is a gradual build-up of buffet intensity followed by a gradual decline as the low-lift buffet region is traversed. This build-up was noted in reference 1 and is illustrated in figure 10 with

qualitative data from the present tests which show the magnitude of the buffet oscillation ΔC_N plotted against Mach number. Also shown on figure 10 are sketches illustrating how these data were reduced by fairing the mean trim lines and the envelopes of the buffet oscillations obtained from the accelerometers of the present tests. The trends thus obtained are believed reliable, although the absolute values of ΔC_N may be inaccurate due to difficulties in fairing the accelerometer records and because of the approximate nature of the amplitude response corrections for high-frequency data.

Drag

Variations of total drag coefficients, based on total exposed wing area, with Mach number are shown on figure 11 for both models together with comparable data from reference 1. The total drag of the model having intersecting surfaces 6 percent thick was higher than the drag of the similar model of reference 1 which had a cruciform arrangement. This increase in drag due to tail position was approximately 17 percent at $M = 1.10$. The total drag coefficient of the model having 12-percent-thick 35° sweptback surfaces was approximately 30 percent lower at $M = 1.00$ than the drag of the model of reference 1 which had 12-percent-thick unswept surfaces. Note, however, that this 30-percent decrease contains not only the effect of sweep but an additional decrease of drag coefficient due to a reduction in streamwise thickness of the swept surfaces from 12 to 10.4 percent and of the vertical surfaces from 7 to 6 percent; hence, the drag decrease due to sweep would be considerably less than the 30 percent indicated above.

CONCLUSIONS

The following conclusions are indicated by the results of flight tests of two rocket-propelled research models:

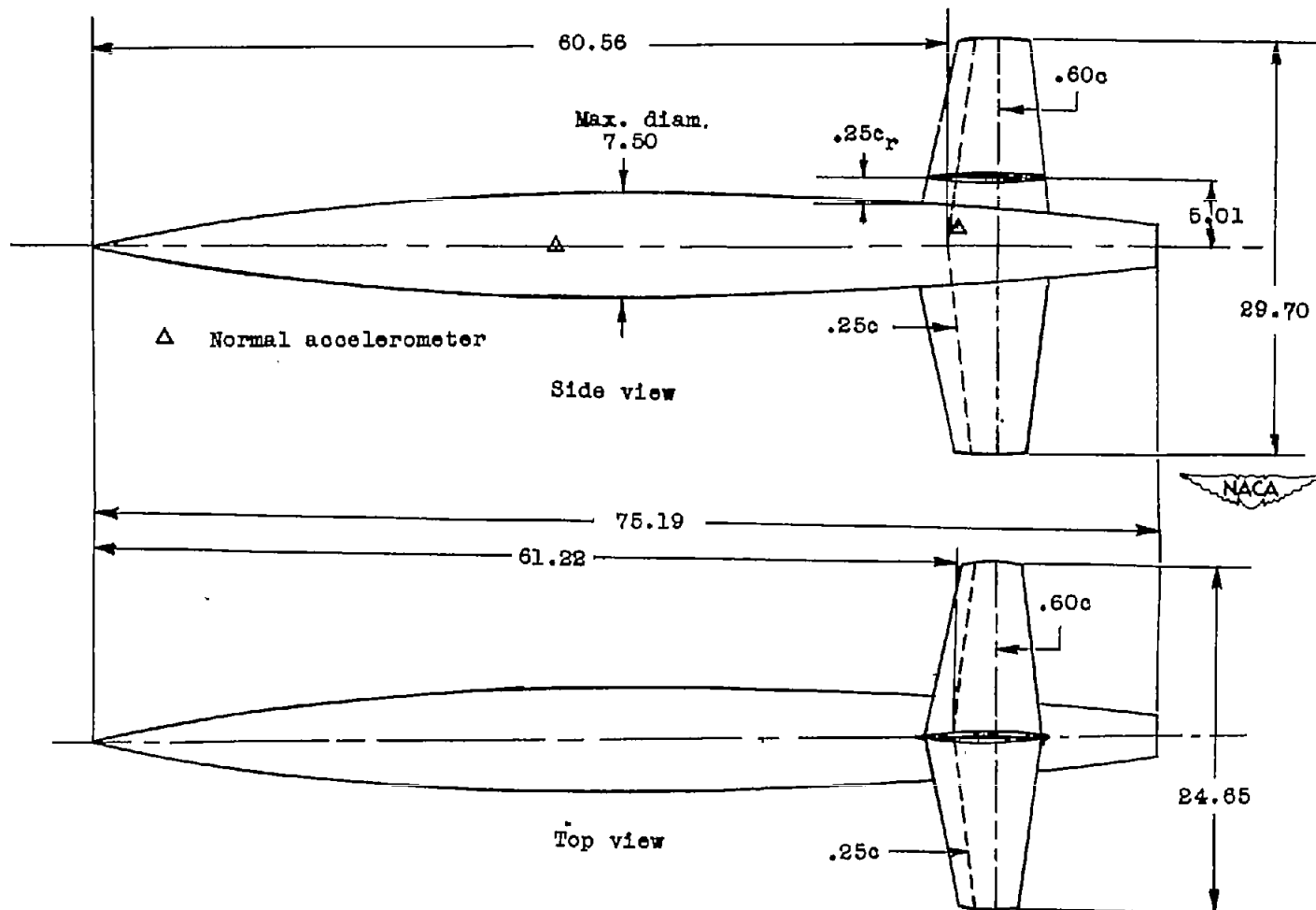
1. Low-lift buffeting may be induced at high subsonic speeds by the interference due to the intersection of thin aerodynamic surfaces.
2. Low-lift buffeting may be alleviated by sweepback; however, 35° sweepback did not eliminate buffeting on the 12-percent-thick surfaces tested.
3. Local interference effects on an intersecting-tail arrangement may be partially responsible for transonic trim changes which persist into the supersonic region.

4. Raising an unswept tail from the body center line to a conventional position on the vertical tail resulted in an appreciable increase in drag at transonic and supersonic speeds.

Langley Aeronautical Laboratory,
National Advisory Committee for Aeronautics,
Langley Field, Va.

REFERENCES

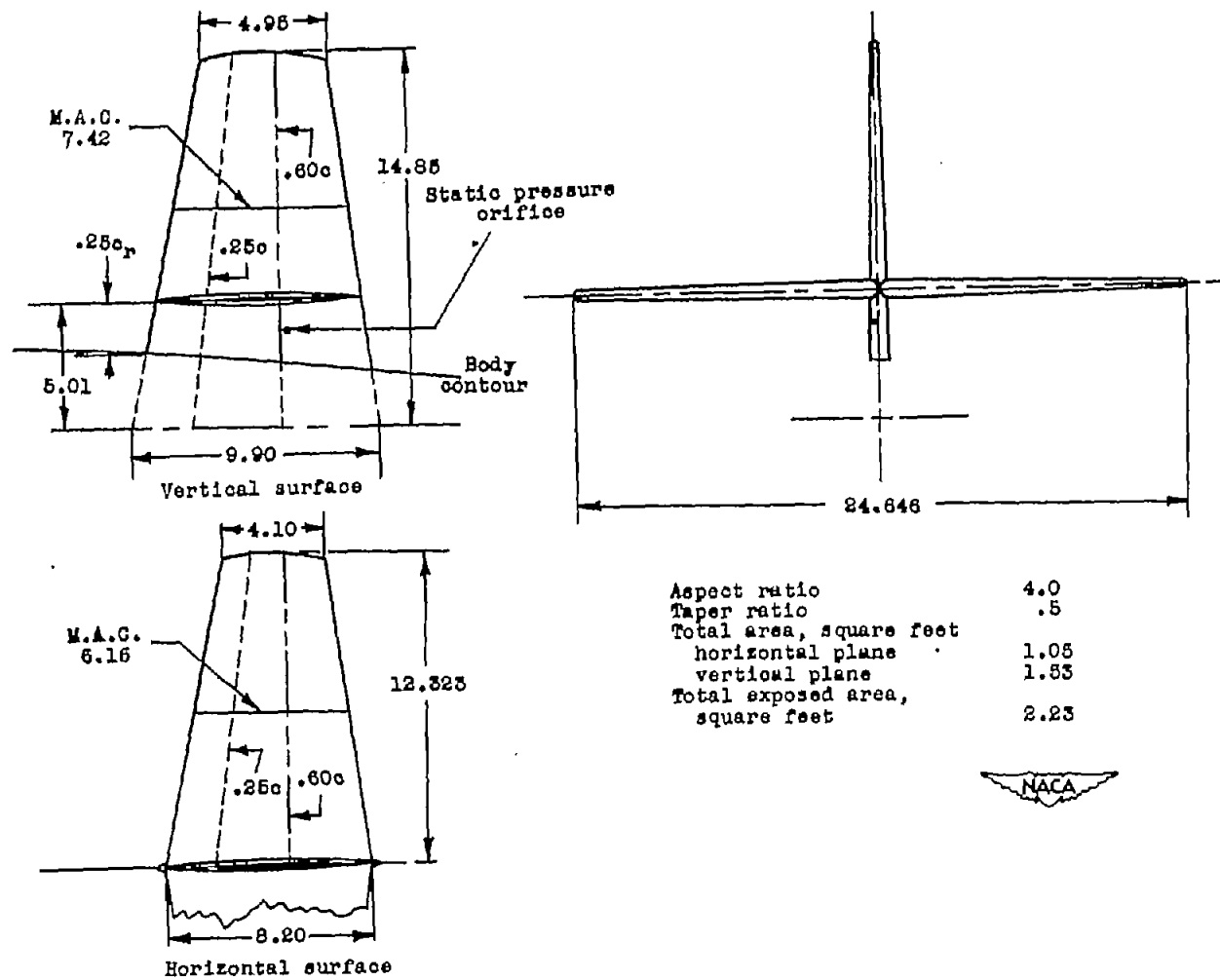
1. Mason, Homer P., and Gardner, William N.: An Application of the Rocket-Propelled-Model Technique to the Investigation of Low-Lift Buffeting and the Results of Preliminary Tests. NACA RM L52C27, 1952.
2. Gadeberg, Burnett L., and Ziff, Howard L.: Flight-Determined Buffet Boundaries of Ten Airplanes and Comparisons With Five Buffeting Criteria. NACA RM A50I27, 1951.
3. Purser, Paul E.: Notes on Low-Lift Buffeting and Wing Dropping at Mach Numbers Near 1. NACA RM L51A30, 1951.
4. Gillis, Clarence L.: Buffeting Information Obtained from Rocket-Propelled Airplane Models Having Thin Unswept Wings. NACA RM L50H22a, 1950.
5. Purser, Paul E., and Wyss, John A.: Review of Some Recent Data on Buffet Boundaries. NACA RM L51E02a, 1951.



CONFIDENTIAL

(a) Complete configuration.

Figure 1.- Specifications of model having 6-percent-thick intersecting surfaces. All dimensions are in inches.

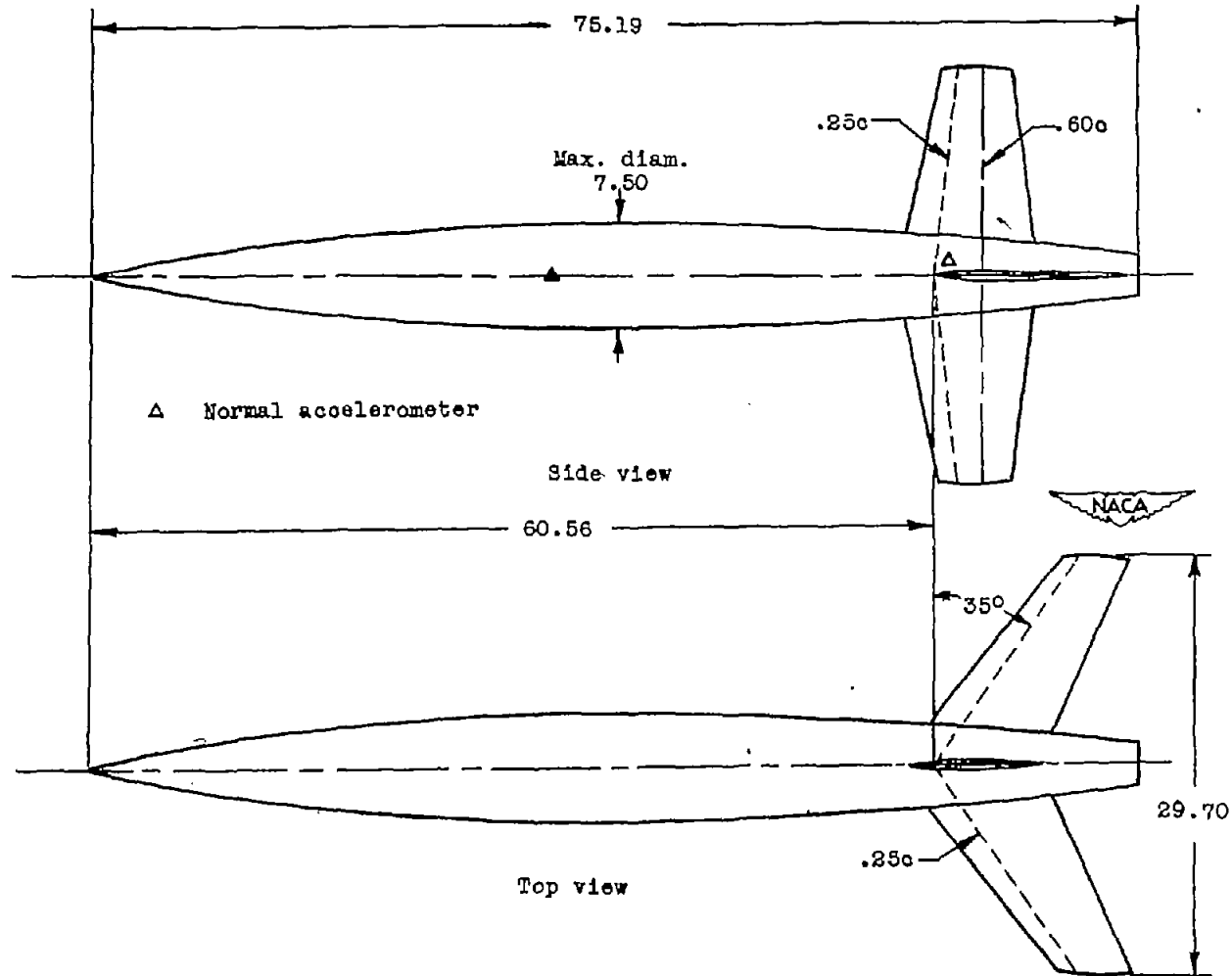


(b) Detail of intersecting surfaces.

Figure 1.- Concluded.

CONFIDENTIAL

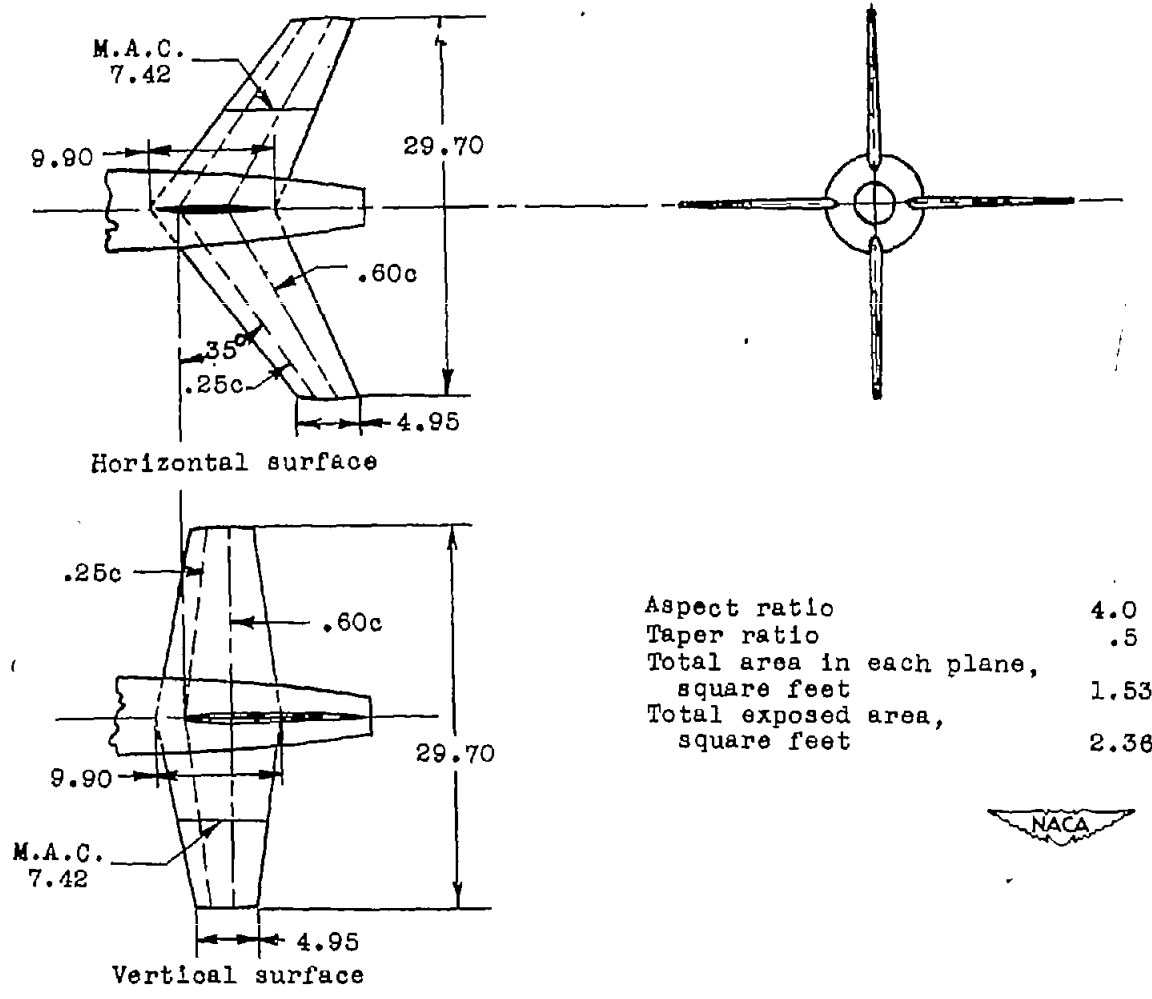
CONFIDENTIAL



CONFIDENTIAL

(a) Complete configuration.

Figure 2.- Specifications of model having 12-percent-thick sweptback surfaces. All dimensions are in inches.

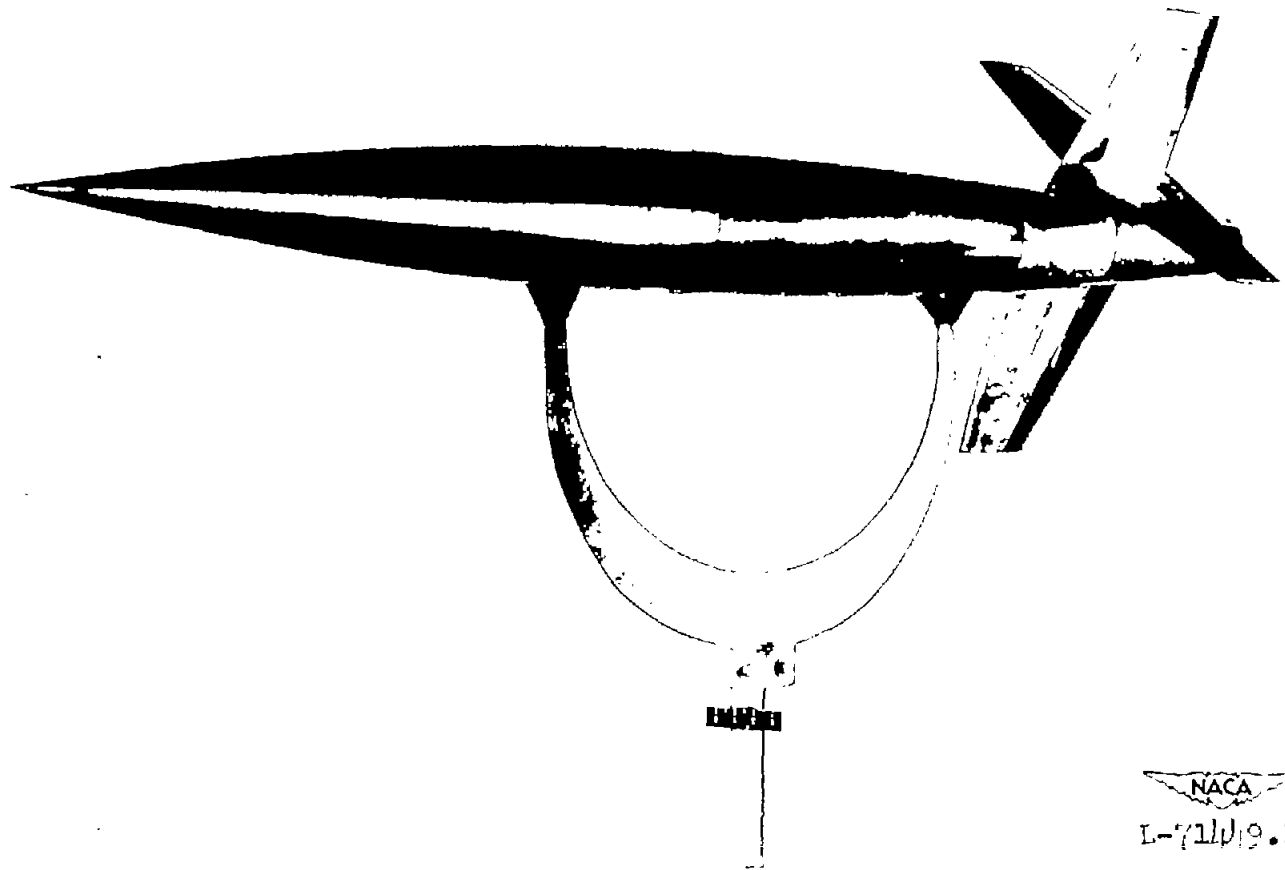


CONFIDENTIAL

(b) Detail of the tail arrangement.

Figure 2.- Concluded.

CONFIDENTIAL

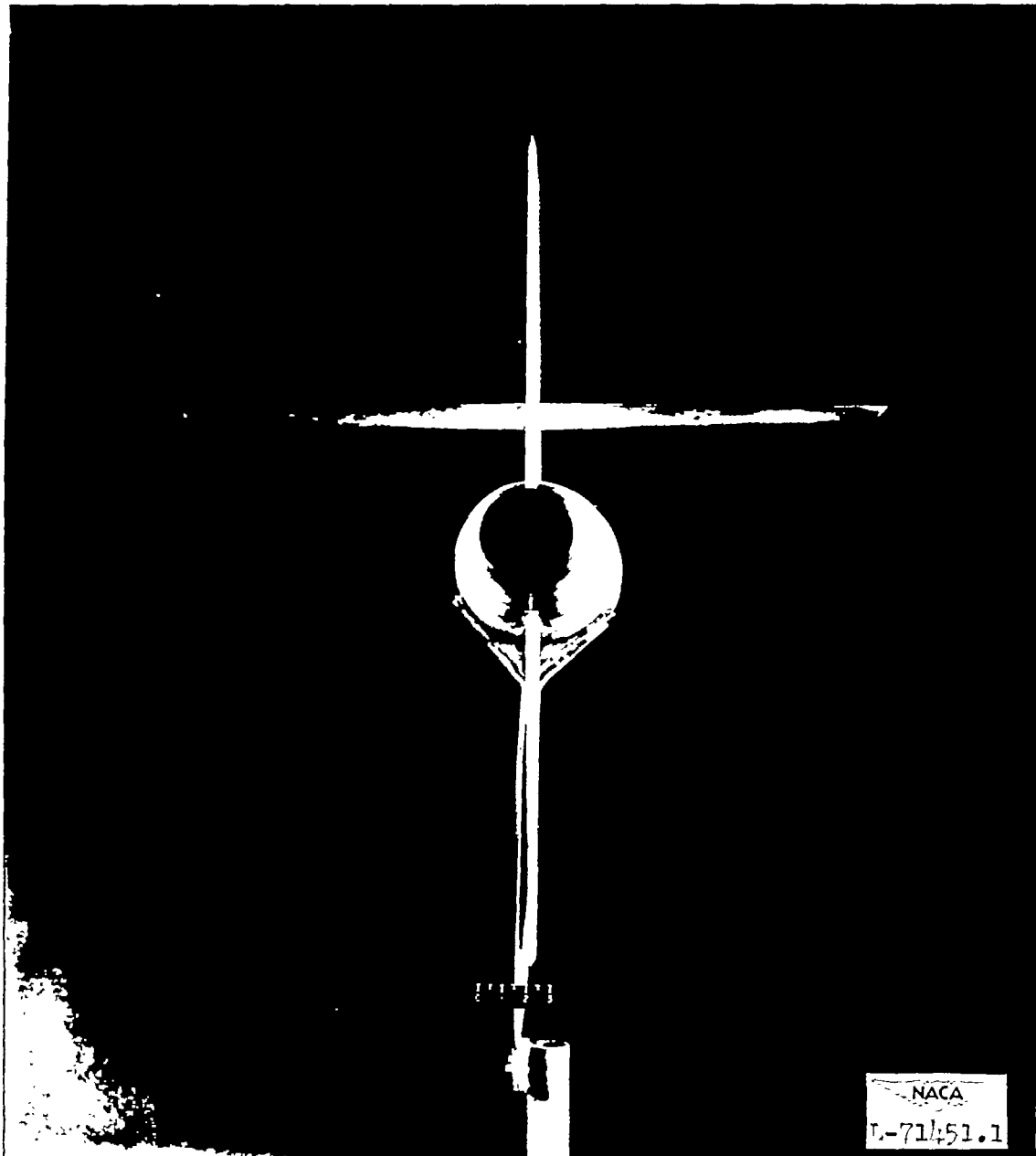


NACA
L-71109.1

(a) Three-quarter front view.

Figure 3.- Photographs of the model having 6-percent-thick intersecting surfaces.

CONFIDENTIAL



(b) Rear view.

Figure 3.- Concluded.

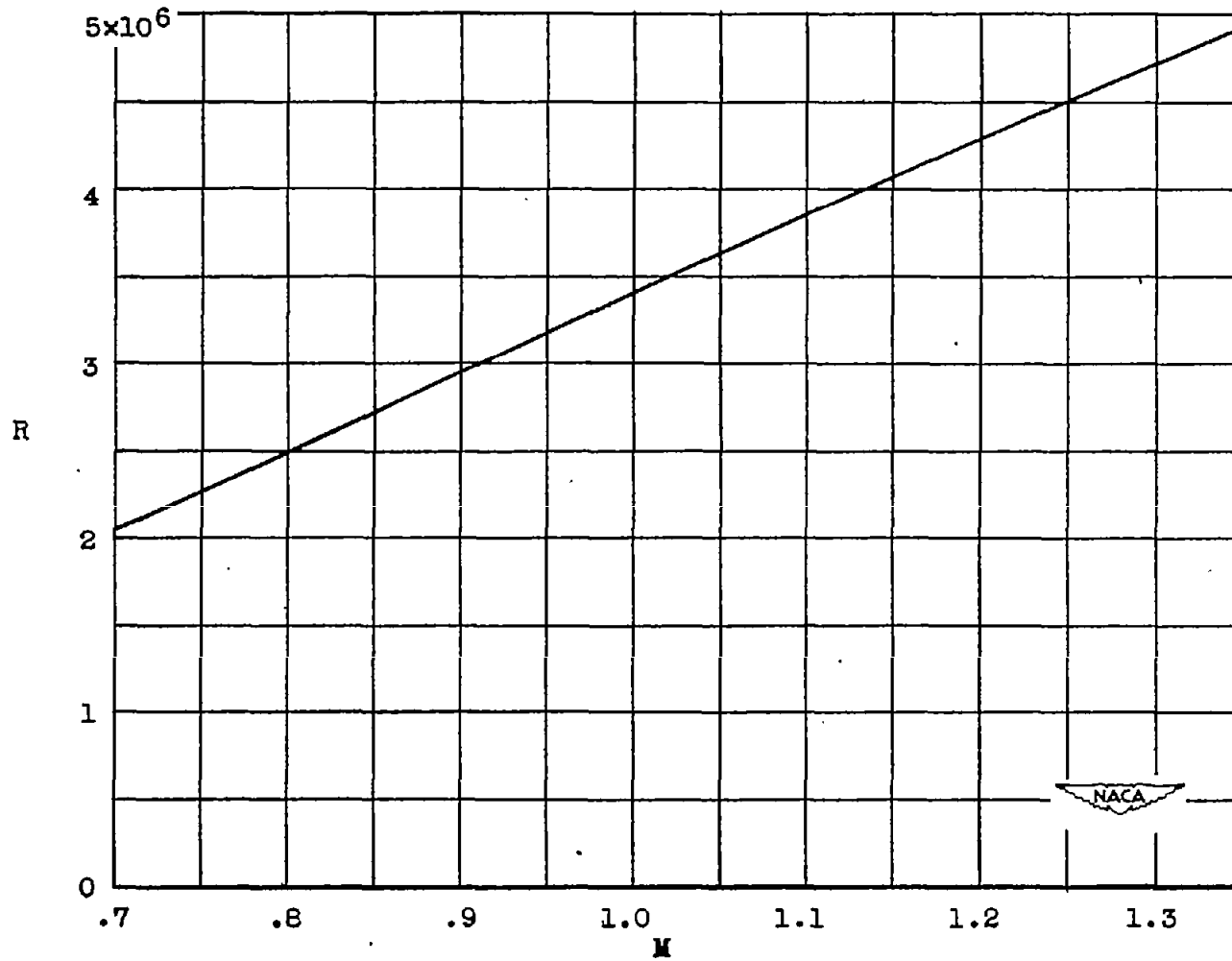


Figure 4.- Variation of Reynolds number with Mach number. Reynolds numbers are based on the mean aerodynamic chord of the vertical surfaces.

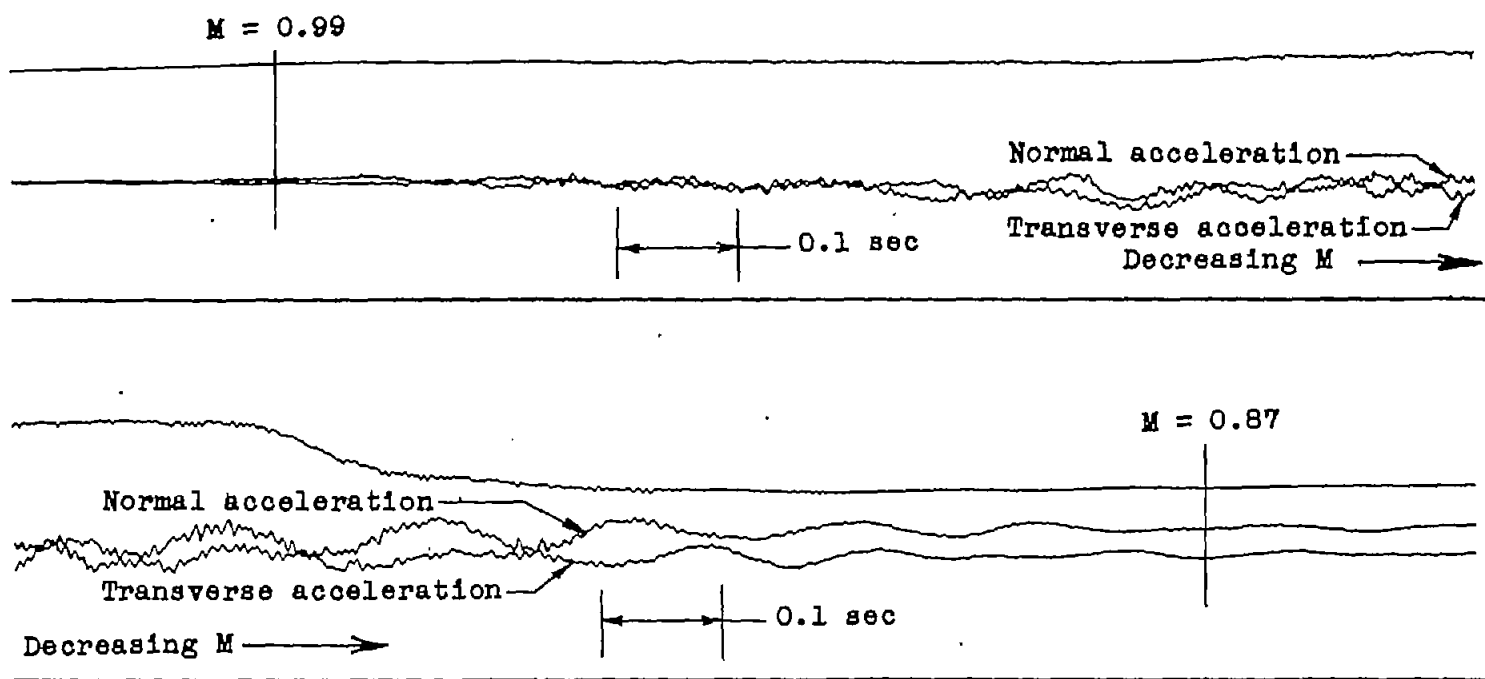


Figure 5.- Part of telemeter record showing accelerations during buffeting of model having thin unswept intersecting surfaces.

CONFIDENTIAL

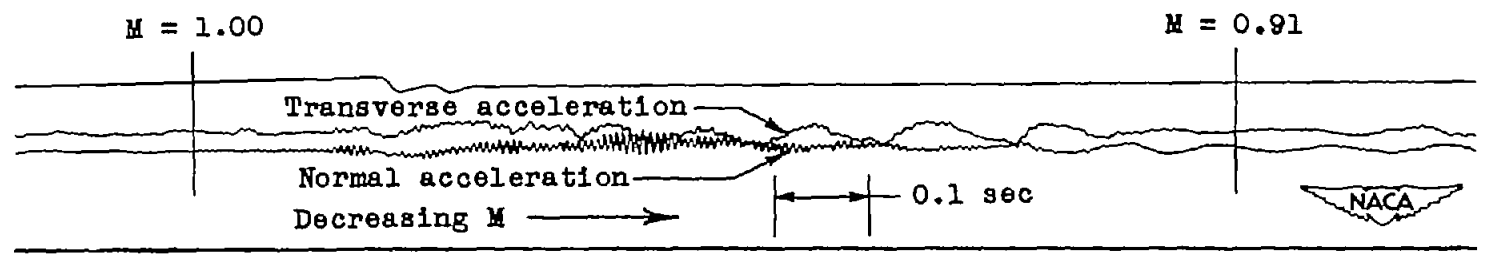


Figure 6.- Part of telemeter record showing accelerations during buffeting of model having thick sweptback surfaces.

CONFIDENTIAL

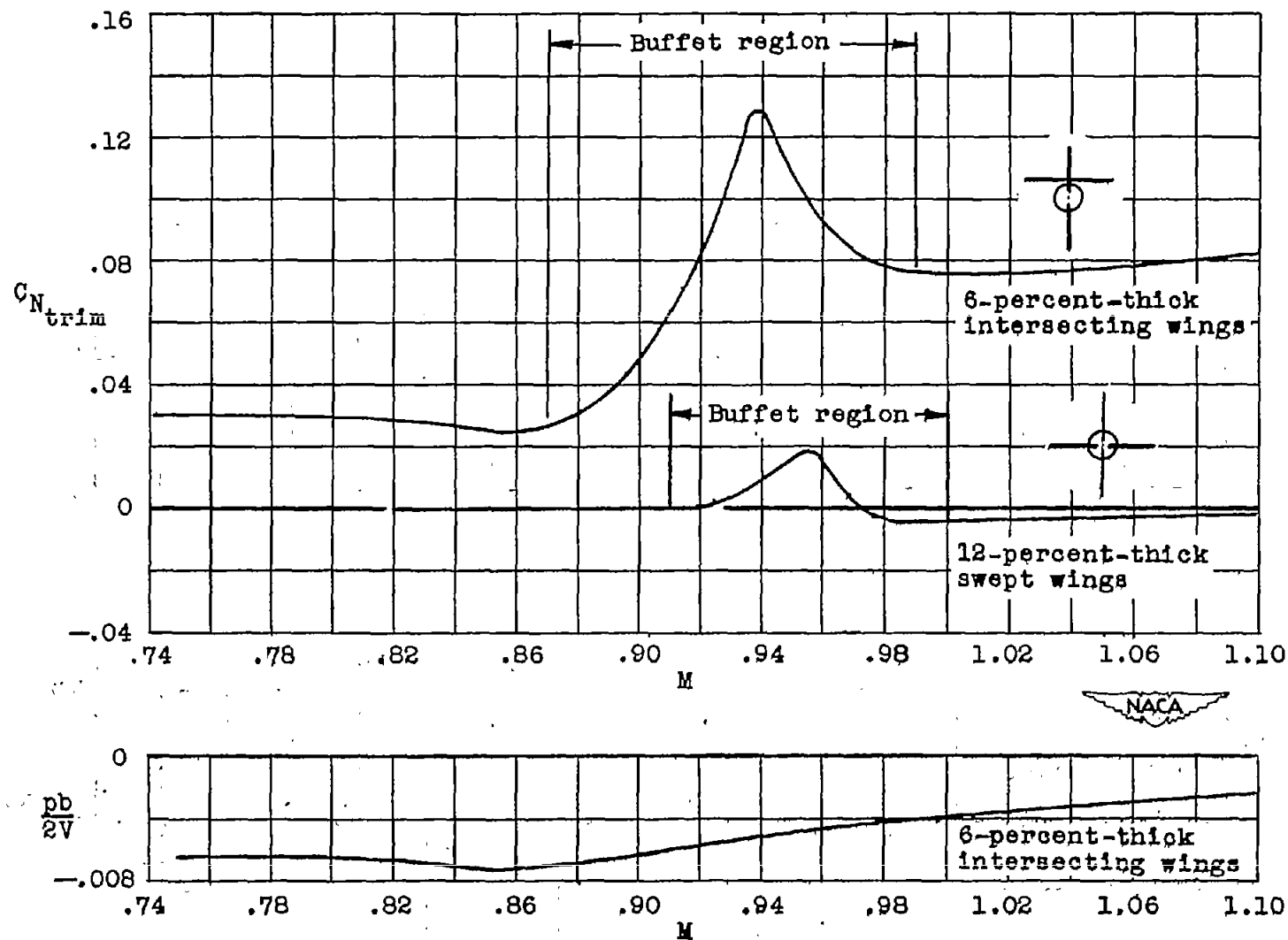


Figure 7.- Variation of trim normal-force coefficients and wing helix angle with Mach number.

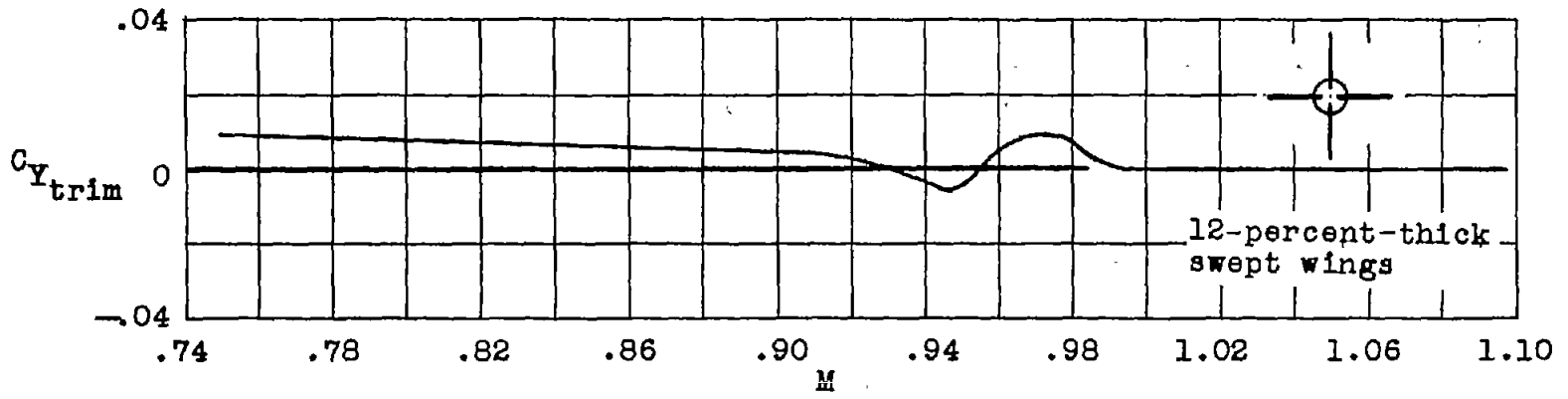
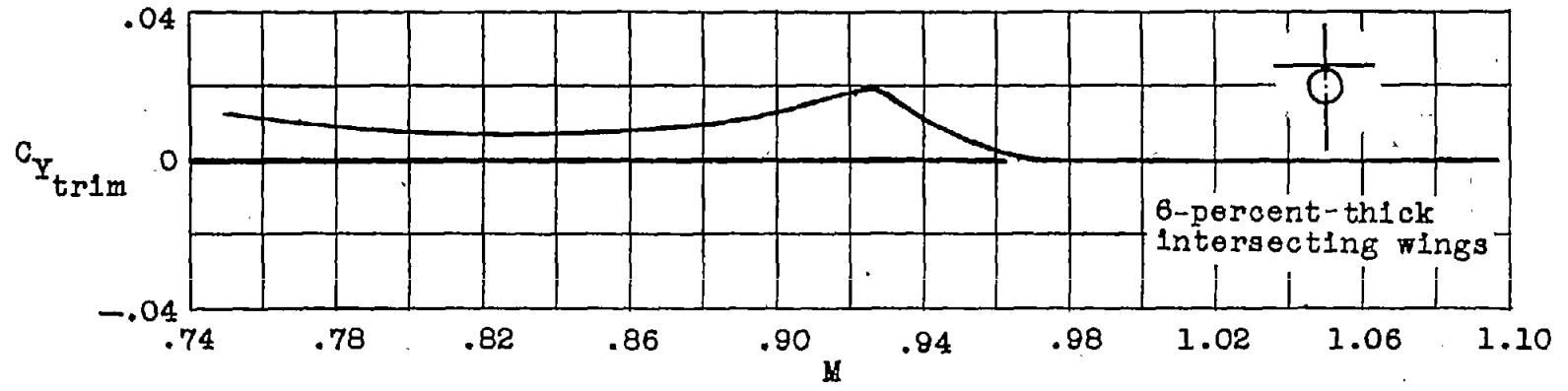


Figure 8.- Variation of trim side-force coefficients with Mach number.

CONFIDENTIAL

CONFIDENTIAL

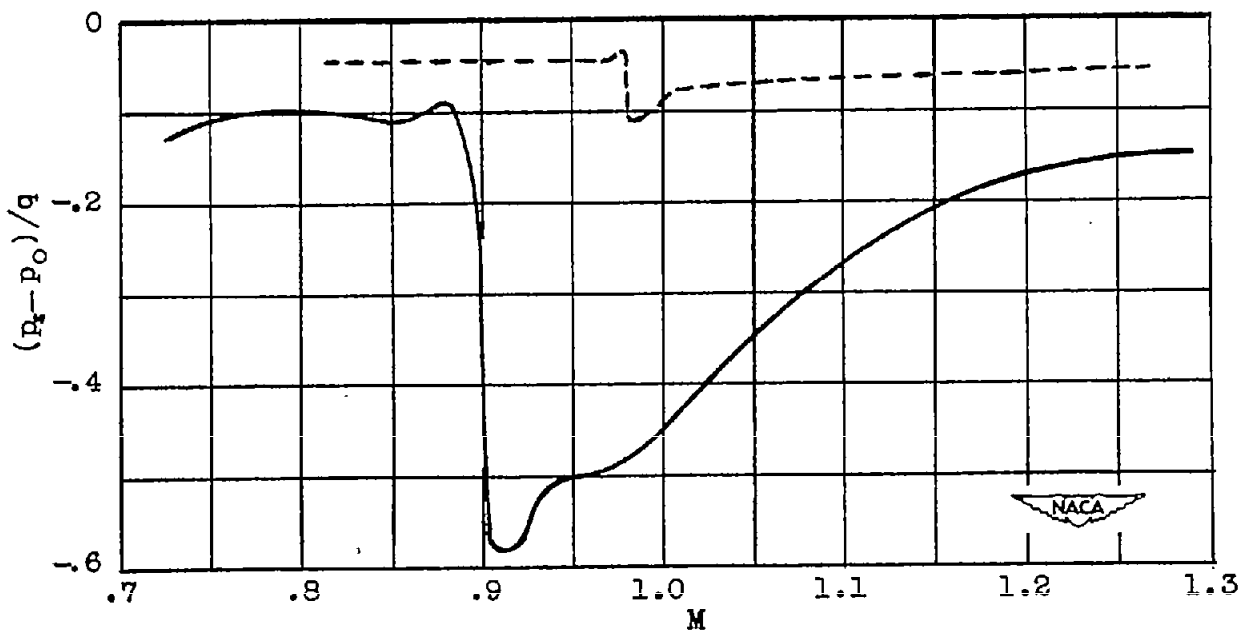
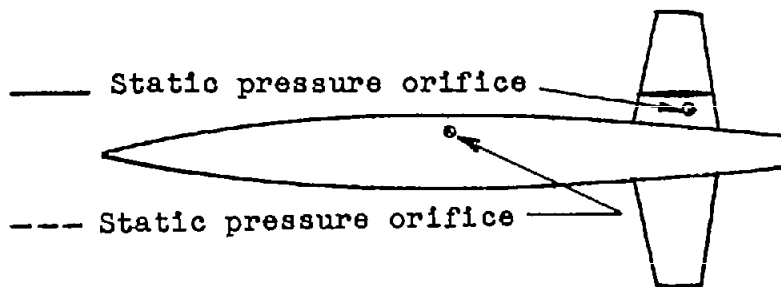
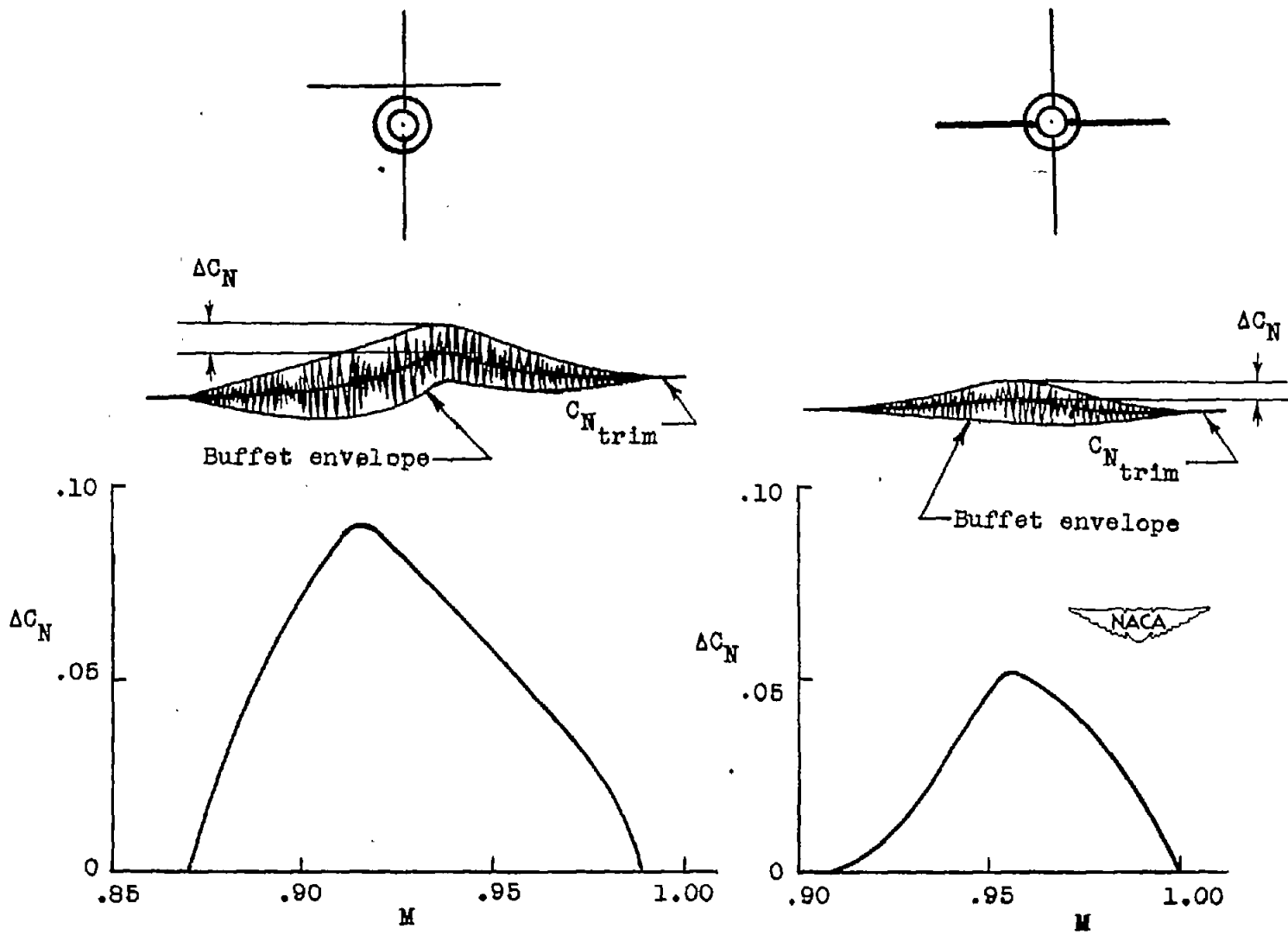


Figure 9.- Variation of static-pressure coefficient with Mach number.

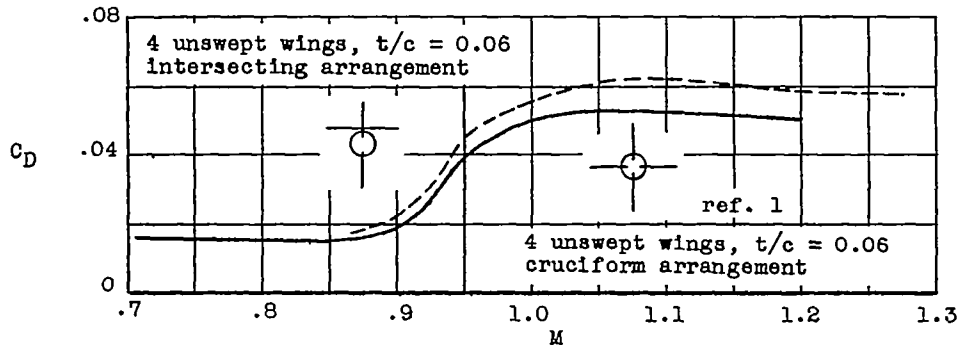
CONFIDENTIAL

CONFIDENTIAL

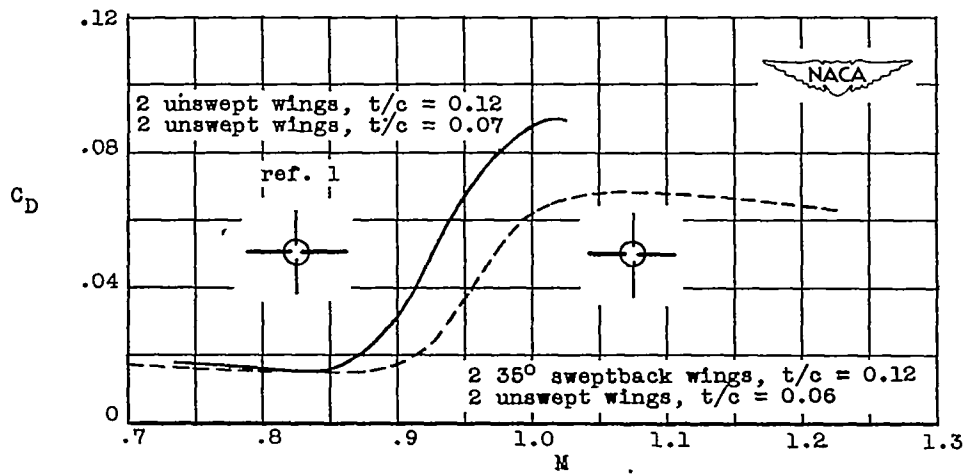


CONFIDENTIAL

Figure 10.- Variation of buffet intensity with Mach number at trim lift.



(a) Effect of tail position.



(b) Effect of sweepback.

Figure 11.— Variation of total drag coefficient with Mach number. All coefficients are based on the total exposed wing area.